Acta Cryst. (1976). A32, 250

X-ray Diffuse Scattering Study of the Low-Temperature Microdomains in Silver β-Alumina

BY J. P. BOILOT, J. THERY AND R. COLLONGUES

Laboratoire de Chimie Appliquée de l'Etat Solide, 11 rue P. M. Curie, 75005 Paris, France

AND R. COMÈS AND A. GUINIER

Laboratoire de Physique des Solides, Université Paris-Sud, 91405 Orsay, France

(*Received* 9 *July* 1975; *accepted* 3 *September* 1975)

A semiquantitative analysis of the X-ray diffuse scattering from β-alumina between 20 K and room temperature shows the change with temperature of the organization of the conducting ions. The earlier-reported low-temperature superstructure never achieves long-range order. Both the size of the 2D domains and the order within the domains, as reflected by the occupation factors, saturate around 77 K. Above this temperature, the size decreases from its saturation value of 45 Å to about 10 Å at 400 K, with a parallel decrease of the order inside the domains. The occupation factors could be determined up to 220 K, and they extrapolate at room temperature to values close to the average occupation determined by conventional structure analysis.

1. Introduction

The β-alumina-type compounds (8·5 Al_2O_3–M_2O) with M = Ag, Na... belong to the new class of materials called superionic conductors (Rice & Roth, 1972). Their conductivity, which is exceptional (Rice & Roth, 1972; Whittingham & Huggins, 1971) for a solid, is due to the two-dimensional diffusion of cations in the low-density layers between the successive spinel blocks which form the construction elements of the bulk crystal structure (Bragg, Gottfried & West, 1931; Roth, 1972; Beevers & Roos, 1937; Peters, Bettman, Moore & Glick, 1971; Reidinger, 1974).

The room-temperature structure determinations showed that these particular electrical properties were related to a structural disorder of the cations. A recent X-ray diffuse scattering study (Le Cars, Comes, Deschamps & Thery, 1974) on silver β-alumina gave a qualitative description of the variation with temperature of the local organization of the silver ions. In this last work, it was established that at high temperature (800 °C), where the ionic conductivity is highest, the silver ions are organized in a two-dimensional quasi-liquid state, and that at low temperature ($T < 300$ K), where the ionic conductivity decreases to values more compatible with a crystalline solid, they tend to form short-range-ordered two-dimensional microdomains.

The present paper is a continuation of this work and its purpose is to describe the results of a systematic X-ray diffuse scattering study between room temperature and 20 K which allow a semi-quantitative analysis of the organization of the conducting silver ions, in the short-range-ordered microdomains. These results establish the variation with temperature of the size of the domains, the positional parameters, the 'apparent' Debye–Waller factors and the occupation factors.

2. Experimental

The single crystals of silver β-alumina were identical to those used in the previous study (Le Cars, Comès, Deschamps & Thery, 1974). They were obtained from sodium β-alumina crystals by molten-salt ion exchange (Yu Yao & Kummer, 1967). Their composition as determined by neutron activation analyses shows an average number of cations of 2·6 per unit cell, *i.e.* 1·3 per unit cell in each low-density layer.

The X-ray diffuse scattering was recorded on photographic films with the technique often improperly described as 'the monochromatic Laue method' (Comès, Lambert, Launois & Zeller, 1973). The intensity of the diffuse scattering on each pattern was measured with a Joyce microdensitometer.

The samples were cooled with a variable-temperature cryocooler ('spectrim' from CTI) and the temperature was regulated to about 0·1 °.

3. Organization of the silver ions at 78 K

In the previous diffuse-scattering study, the site model shown in Fig. 1(*a*) was used for the average disordered structure of the silver ions in the low-density planes; this model was a simplification of the electronic density distribution determined by Roth (1972) and shown in Fig. 1(*b*); with this approximation, two possible schematic structures shown in Figs. 2(*a*) and 2(*b*) were proposed to account for the short-range hexagonal superlattice of the low-temperature microdomains (supercell lattice constant $A = a\sqrt{3} = 9{\cdot}68$ Å, and oriented at 30° from the average cell axis of β-alumina: $a = 5{\cdot}59$ Å) revealed by the X-ray diffuse scattering at 77 K.

These two models are unique if *only one* of the three Ag (1) sites can be occupied in the low-density layer

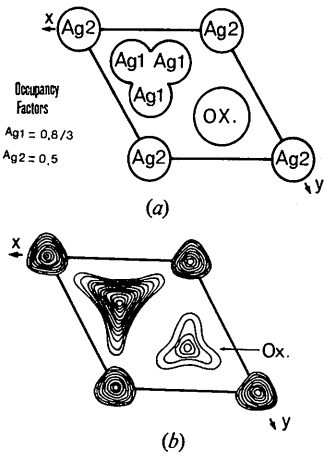

Fig. 1. Approximation for the average structure unit-cell (*a*) deduced from the electronic distribution shown in (*b*).

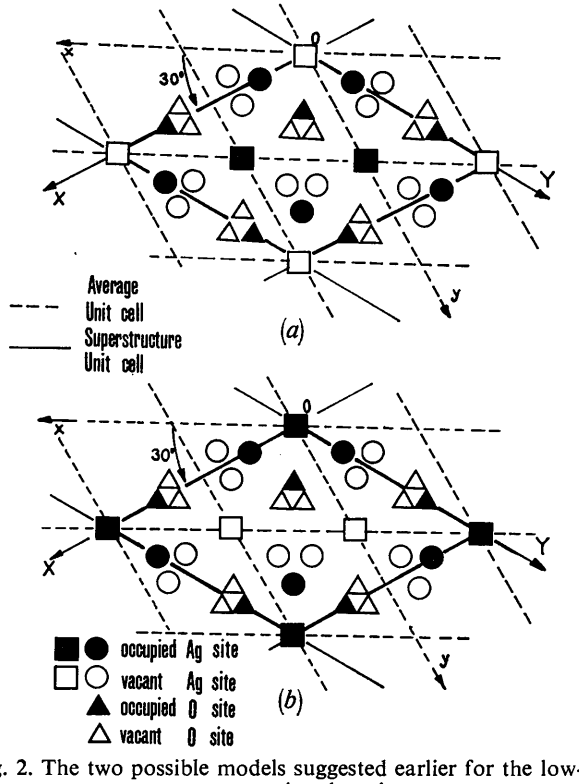

Fig. 2. The two possible models suggested earlier for the low-temperature microdomains.

of a given unit cell. Such an assumption is justified by the size of the silver ions and the value of the positional parameter of the Ag (1) ions in the average structure as reflected by the extension of the spikes of the electronic density distribution around the Ag (1) positions [Fig. 1(*b*)].

The first aim of our analysis was to choose between the two structures shown in Fig. 2.

For any type of disorder (chemical disorder or displacive disorder, *i.e.* phonons), the intensity of the diffuse scattering is proportional to the mean-square deviation from the average structure determined by conventional diffraction analysis.

In order to perform our calculation, the different low-temperature microdomains were taken as incoherent relative to one another; the total scattered intensity is then the sum of the intensities scattered by each individual microdomain. It is therefore sufficient to limit the calculation to one microdomain. Doing this, we look at the problem of β-alumina from the low-temperature side, and treat the microdomain as a small crystal or what we could call 'long short-range order'. The scattered intensity is then proportional to I_d given by:

$$I_d = \langle F_{cd} \rangle^2 = \langle F - \langle F \rangle \rangle^2 \exp(-2M)$$

where

– F_{cd} is the calculated structure factor for the short-range order in a superstructure unit cell accounting for the diffuse scattering,

– F is the structure factor of one low-temperature superlattice unit cell using the models of Fig. 2,

– $\langle F \rangle$ is the *average* structure factor of the same superlattice unit cell, that is to say that we use all sites and occupancy factors of the approximate average structure of Fig. 1(*a*) which are located in one superlattice unit cell,

– The Debye–Waller factor $M = [(H^2 + K^2)\beta_{11} + 2HK\beta_{12}]10^{-4}$ is anisotropic, but has been taken as identical for all atoms. Considering the limited number of experimental data which can be collected with such diffuse scattering experiments (a typical order of magnitude for the intensity of diffuse scattering compared to ordinary Bragg reflexions goes from 10^{-2} to 10^{-3}), it was felt unreasonable to introduce several temperature factors.

To avoid contamination from the Bragg reflexions of the average structure, we have taken into account

Table 1. *Occupation factors*

	Wyckoff positions of the 2D space group $p31m$	Occupation factors For local structure factor F Model (*a*)	Model (*b*)	For average structure factor $\langle F \rangle$
Ag(1)	3(*c*)	1	1	0·8/3
	6(*d*)	0	0	0·8/3
Ag(2)	1(*a*)	0	1	0·5
	2(*b*)	1	0	0·5
Oxygen	3(*c*)	1	1	1/3
	6(*d*)	0	0	1/3

only the superstructure diffuse spots in the agreement index:

$$R = \frac{\sum |F_{obs} - F_{cd}|}{\sum F_{obs}}$$

and made a qualitative check of the agreement between the calculated values F_{cd}, and the observed values (always weak) of the diffuse spots coinciding with these Bragg reflexions.

We recall here that the low-dimensional order is 2D, which means that the diffuse scattering due to the domains forms diffuse rods parallel to the c axis. When we talk in terms of diffuse spots, we refer to a pattern performed with the c axis of the sample parallel to the incident X-ray beam, on which, owing to the intersection of the rods with the Ewald sphere, only diffuse spots are observable.

With the occupation factors listed in Table 1, a refinement on the positional parameters of the Ag (1) ion and the oxygen ion which were allowed to vary only within the narrow limits compatible with the average electronic density distribution [the position of the Ag (2) ion for instance is determined by the average structure], and a refinement of the temperature factors, we get an R of 0·36 for model (*a*) [Fig. 2(*a*)] and of 0·16 for model (*b*) [Fig. 2(*b*)].

The model (*b*), which corresponds to 1·33 silver atoms per average unit cell and is the closest to the average concentration of 1·30 per average unit cell, is obviously better than model (*a*). This is in agreement with the absence of small-angle scattering (at room temperature) mentioned by Le Cars *et al.* (1974). Unfortunately, the refined model gives calculated values F_{cd} for the diffuse spots coinciding with average Bragg reflexions which are large compared to the observed values.

This discrepancy led us to a more complex model (*b'*) close to model (*b*) but which is only partially ordered; the occupation factors for the silver ions were allowed to take values smaller than one for the 3(*c*) and 1(*a*) positions [model (*b*)], and non-zero values for the 6(*d*) and 2(*b*) positions [model (*a*)], and were also refined.

Table 2 shows the positional parameters, the occupation factors, and the Debye–Waller (DW) factors which gave the best agreement index of $R = 0{\cdot}07$ for the superstructure diffuse spots

Table 3 gives the observed and calculated amplitudes, for the superstructure diffuse spots [Table 3(*a*)] and for the diffuse spots centred on the Bragg reflexions of the average structure [Table 3(*b*)]. It can be

Table 2. *Model* (*b'*)–78 K

	2D Wyckoff positions	Occupation factor	x	y	Factors β_{11}	β_{12}
Ag(1)	3(*c*)	0·58	0·22	0		
	6(*d*)	0·21	0·44	0·11		
Ag(2)	1(*a*)	0·69	0	0	80	70
	2(*b*)	0·31	0·33	0·66		
O	3(*c*)	1	0·88	0		

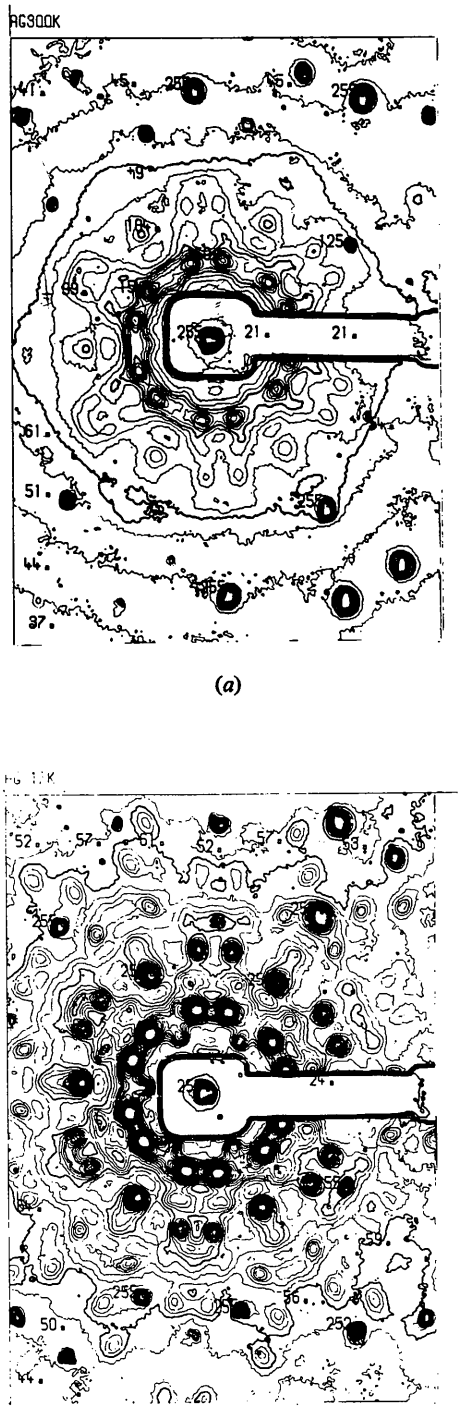

(*a*)

(*b*)

Fig. 3. Iso-intensity curves of patterns produced at 300°K (*a*) and at 20°K (*b*). These curves were recorded with an Optronics photoscan system P-1000 (Service National du Microdensitomètre, – Bât. 510, Orsay, France). The β-alumina crystal is oriented with its c axis parallel to the incident beam.

seen that the agreement, even for this last series of data, which was not used in the refinement, is quite good.

Table 3. *Observed and calculated amplitudes*

	H	K	$\lvert F_{obs}\rvert$	$\lvert F_{cal}\rvert$
(*a*) Superstructure	0	4	36	36
diffuse spots used	1	2	32	32
in the refinement	2	3	24	19
$R=0{\cdot}07$	0	2	11	12
	3	4	13	13
	4	5	16	16
	2	6	15	15
	1	6	14	17
	1	5	16	17
	5	6	4	4
	3	7	9	9
	2	7	6	3
(*b*) Diffuse spots	0	3	Weak	4
coinciding with	0	6	Very weak	0·3
average Bragg reflex-	1	4	Weak	5
ions which were not	1	7	6	7
included in the refine-	4	4	4	3
ment	3	6	Very weak	2

With 12 independent and reliably measured intensities (superstructure, diffuse spots) and nine adjustable parameters [including the only partially adjustable position parameters of the Ag (1) and oxygen ions] the result of model (*b'*) was considered to be the limit of what could be reliably expected from such an analysis of the diffuse scattering from the short-range-ordered microdomains at 77 K.

The same model (*b'*) was used to analyze the temperature variation of the different parameters.

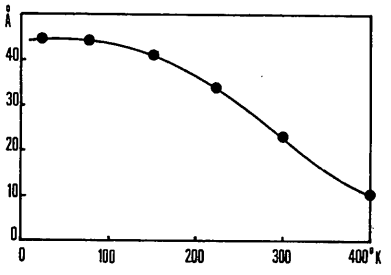

Fig. 4. Temperature variation of the size of the superlattice microdomains.

4. Change with temperature of the size and structure of the microdomains

To recall the aspect of the scattering patterns and their evolution with temperature, Fig. 3 shows the iso-intensity curves of patterns produced at room temperature [Fig. 3(*a*)] and at 20 K [Fig. 3(*b*)] which were microscanned. It clearly shows the formation of superstructure diffuse spots, which are best defined at the lowest temperature, but which already emerge at room temperature for the most intense ones.

Assuming that the different 2D microdomains have roughly the same size (at a given temperature), the average size (perpendicular to **c**) of the short-range-ordered domains can be deduced from the full width at half maximum of the diffuse spots. Fig. 4 shows this size as a function of temperature. Saturated around 45 Å below 100 K, it decreases with increasing temperature above 100 K to reach a value of about the superstructure unit cell (9·68 Å) around 400 K. Independently, from the fact that only a few diffuse spots are still visible at 300 and 400 K, the small sizes reached in the upper part of the temperature range show that it is impossible to analyze the diffuse intensity due to the local order with the small-crystal approximation. Our results are therefore restricted to the lower temperatures (20 to 220 K).

Table 4 shows the evolution with temperature of the occupational parameters and of the temperature factors.

As was already found for the evolution of the size of the short-range-ordered regions, little change is observed below 100 K, the structural parameters start to change above 100 K towards their average value (Fig. 5). Striking is the difference of the evolution of the thermal parameters β_{11} and β_{12}; β_{11} corresponds indeed to a motion of the atoms in the directions of the spikes of the electronic density distribution around the Ag (1) ions found for the average structure [Fig. 1(*b*)], *i.e.* to the direction of easy ionic diffusion responsible for the high electrical conductivity.

The highest temperature at which the analysis could be performed is 220 K. A rough estimate of the room-temperature occupation factors can be obtained by extrapolation from the low-temperature results (Fig. 5). Such an extrapolation indeed yields values around

Table 4. *The average size of the short-range-ordered domains as a function of temperature*

	Wyckoff position	20 °K Q*	20 °K $\langle\beta_{11}\rangle$	20 °K $\langle\beta_{12}\rangle$	78 °K Q*	78 °K $\langle\beta_{11}\rangle$	78 °K $\langle\beta_{12}\rangle$	150 °K Q*	150 °K $\langle\beta_{11}\rangle$	150 °K $\langle\beta_{12}\rangle$	220 °K Q*	220 °K $\langle\beta_{11}\rangle$	220 °K $\langle\beta_{12}\rangle$	Recall of RT average structure Q*	Recall of RT average structure $\langle\beta_{11}\rangle$	Recall of RT average structure $\langle\beta_{12}\rangle$
	3(*c*)	0·60	↑	↑	0·58	↑	↑	0·50	↑	↑	0·44	↑	↑	0·266	↑	↑
Ag(1)	6(*d*)	0·20	|	|	0·21	|	|	0·23	|	|	0·24	|	|	0·266	|	|
			50	60		80	70		180	120		320	170		523	261
Ag(2)	1(*a*)	0·71	↓	↓	0·69	↓	↓	0·60	↓	↓	0·54	↓	↓	0·5	↓	↓
	2(*b*)	0·29			0·31			0·40			0·46			0·5		
N_{Ag}†			1·43			1·437			1·427			1·407			1·30	
R			0·07			0·07			0·08			0·12				

* Q = occupation factor.
† N_{Ag} = Number of Ag ions per average unit cell.

300 K which are very close to the average occupation, confirming the statement made above that another type of analysis must be used above 300 K.

In contrast with the occupational parameters and the temperature factors, no significant change is observed on the positional parameters of the Ag (1) ions and the oxygen ions. As far as these ions are concerned, this result implies that their positional parameters in the *average structure* are independent of temperature and that the major changes affect the temperature factors – and eventually the average occupation factors. The low-temperature structure determination of sodium β-alumina by Reidinger (1974) yields a similar conclusion.

5. Discussion

We have shown that the diffuse scattering patterns of Ag β-alumina at low temperature could be reasonably well explained by the formation of partially ordered microdomains of about 45 Å, corresponding to the short-range superstructure described above as model (*b'*), with occupational parameters and temperature factors varying with temperature. In this model we have not taken into account a possible coupling of the short-range order in the low-density planes with the closest oxygen or aluminum atoms from the spinel blocks. Such a coupling would modulate the intensity along the diffuse rods (*l* direction), and possibly affect the measured intensities for the higher *h* and *k* values. This could therefore slightly modify the model. Another general assumption of the trial models (*a*), (*b*), (*b'*) for the short-range superstructure, was to limit the possible Ag (1) sites to one per average unit cell, and to use the simplified average structure shown in Fig. 1(*a*) which does not have a mid-oxygen site ($x=\frac{2}{3}$; $y=\frac{1}{3}$). Unless the average structure, which is presently only known precisely at room temperature, is drastically modified at low temperature, none of the above mentioned limitations should seriously modify the overall agreement of model (*b'*) with the observed scattering pattern. One surprising aspect of model (*b'*) is that the atoms in the Ag (1) site relax toward an occupied Ag (2) site which results in clusters of four Ag ions at the origin of the superlattice cell.

In the preceding paragraphs we have treated the structural variations observed at low temperature in silver β-alumina in terms of static effects, but, as is well known, X-rays cannot distinguish static from dynamical effects. Considering the small size of the so-called 'low-temperature microdomains' even at the lowest temperatures (here 20 K), it may be more appropriate to talk in terms of fluctuations. This does not change the structural calculations, but may throw some light on the variations with temperature of the different parameters.

One may be tempted as suggested by B. A. Huberman (Private communication) to treat the 'low-temperature microdomains' as fluctuations into droplets of diameter ξ, whose free energy density has the usual form:

$$F(\psi)=\alpha|\psi|^2+\beta|\psi|^4+c\left|\frac{d\psi}{dr}\right|^2.$$

For a scalar order parameter in 2D, the correlation length goes like $1/\alpha$, *i.e.* the diameter ξ of the droplets should go like $(T-T_0)^{-\nu}$ with $\nu=1$ and T_0 a hypothetical phase-transition temperature. If we try to apply such an approach to the higher-temperature measurements (400 K, 300 K) of Fig. 4, it leads to a value of T_0 of about 220 K. As seen above, the different structural parameters do not show such a phase transition, but instead, after a relatively rapid change in the temperature range between 400 and 150 K, they all saturate around the value reached at 80 K – only short-range order can be achieved in Ag β-alumina.

This absence of a real phase transition in β-alumina is in remarkable contrast with the observations on other superionic conductors such as $RbAg_4I_5$ (Owens & Argue, 1967) or $(C_5H_5NH)Ag_5I_6$ (Geller & Owens, 1972) in which the conducting Ag^+ ions reach long-range order respectively below −155°C and −30°C, but all these other examples are stoichiometric compounds while β-alumina is not.

With the composition of our samples assuming total ion exchange, *i.e.* 1·3 silver atoms per average unit cell in each low-density layer, there are indeed not enough silver atoms to extend the low-temperature superlattice (which corresponds to 1·43 Ag^+ ions per average unit cell in each low-density layer) over the whole crystal. If the stability of the bulk crystal on the other hand requires a minimum local concentration of Ag^+ ions, it is understandable that the size of the ordered droplets is bound to an upper limit. It would therefore be of great interest to compare samples of variable composition; β-alumina has indeed been found to exist in the range 5·33 Al_2O_3–Ag_2O to 8·5 Al_2O_3–Ag_2O, with an ionic conductivity decreasing with increasing silver content, which would be con-

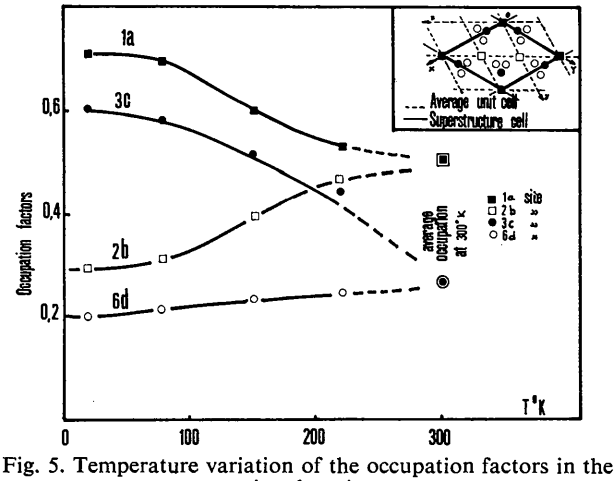

Fig. 5. Temperature variation of the occupation factors in the microdomains.

sistent with a greater order, *i.e.* large superstructure domains themselves more perfectly ordered.*

Conclusion

The conclusions of the present study of β-alumina with a composition of 8·3 Al_2O_3–Ag_2O are:

(i) That the low-temperature superstructure arising from the conducting ions never achieves long-range order and saturates around liquid-nitrogen temperature into domains of about 45 Å diameter.

(ii) That even in these short-range superstructures, the order is not complete, decreases with increasing temperature and extrapolates, around room temperature, to values close to the average occupation determined by conventional structure analysis.

We are grateful to D. B. McWhan and S. M. Shapiro for fruitflu discussions and to L. Deschamps for his efficient technical help during the low-temperature experiments.

* Just after this work had been submitted for publication, we received a preprint on the ion–ion correlation and diffusion in several β-alumina-type compounds (McWhan, Allen, Remeika & Dernier, 1975), which yields somewhat different results. Noteworthy is the fact that the Na β-alumina crystals (which are the starting material) used have been grown from a flux and have a slightly different composition ($1{\cdot}6Na_2O.11Al_2O_3$ compared to our $1{\cdot}33Na_2O.11Al_2O$). This could be directly relevant to the present discussion.

References

BEEVERS, C. A. & ROOS, M. A. S. (1937). *Z. Kristallogr.* **97**, 59–66.

BRAGG, W. L., GOTTFRIED, C. & WEST, J. (1931). *Z. Kristallogr.* **77**, 255–274.

COMÈS, R., LAMBERT, M., LAUNOIS, H. & ZELLER, H. R. (1973). *Phys. Rev.* B**8**, 571–575.

GELLER, S. & OWENS, B. B. (1972). *J. Phys. Chem. Solids*, **33**, 1241–1250.

LE CARS, Y., COMÈS, R., DESCHAMPS, L. & THERY, J. (1974). *Acta Cryst.* A**30**, 305-309.

MCWHAN, D. B., ALLEN, S. J. JR, REMEIKA, J. P. & DERNIER, P. D. (1975). *Phys. Rev. Lett.* **35**, 953.

OWENS, B. B. & ARGUE, G. R. (1967). *Science*, **157**, 308–309.

PETERS, C. R., BETTMAN, M., MOORE, J. W. & GLICK, M. D. (1971). *Acta Cryst.* B**27**, 1826–1834.

REIDINGER, F. (1974). Unpublished, referred to by W. L. ROTH, General Electric Rep. No. 74CRDO54, March 1974.

RICE, M. J. & ROTH, W. L. (1972). *J. Solid State Chem.* **4**, 294–310.

ROTH, W. L. (1972). *J. Solid State Chem.* **4**, 60–75.

WHITTINGHAM, M. S. & HUGGINS, R. A. (1971). *J. Chem. Phys.* **54**, 414.

YU YAO, Y. F. & KUMMER, J. T. (1967). *J. Inorg. Nucl. Chem.* **29**, 2455–2475.

Acta Cryst. (1976). A**32**, 255

Test Refinements with Simulated Protein Data Sets

BY R. E. STENKAMP AND L. H. JENSEN

Department of Chemistry and Department of Biological Structure, University of Washington, Seattle, WA. 98195, U.S.A.

(*Received* 27 *June* 1975; *accepted* 26 *September* 1975)

The method of differential difference syntheses combined with idealization for refining protein models has been tested on a dipeptide derivative. An r.m.s. error of 0·5 Å was introduced in the dipeptide model, and the data were modified by applying artificial temperature factors to simulate the case of a protein. In any one of several variations, differential difference syntheses with idealization led to convergence at *R* values substantially lower than for proteins, but refinement is slow, requiring many cycles.

Two methods of refining a protein model based on X-ray diffraction data are by difference syntheses (Watenpaugh, Sieker, Herriott & Jensen, 1973) and by differential difference syntheses combined with application of constraints to maintain acceptable bond lengths, interbond angles and certain torsion angles (Freer, Alden, Carter & Kraut, 1975). To check the differential difference method with the application of constraints we have undertaken a series of test refinements using a small-molecule data set limited and modified to simulate that of a protein. These tests offer two advantages: (1) the parameters from the test refinements can be compared with accurate values from the conventional refinement, and (2) because the test case is small relative to a protein structure, it is economically feasible to compare variations of the basic method of refinement.

Test refinement

The structure chosen for the test was *N*-acetyl-L-phenylalanyl-L-tyrosine (NAPT) (Stenkamp & Jensen, 1973). Table 1 contains relevant crystal, refinement, and data set information. The data set was truncated at *d* spacings typical of high-resolution protein data that